Infrasonic estimation of surf period

Jérôme Aucan,[1] David Fee,[2] and Milton Garcés[2]

Received 29 October 2005; revised 7 December 2005; accepted 21 December 2005; published 10 March 2006.

[1] Synchronous infrasonic, video, and wave height measurements were performed during high surf at Polihale beach, Kauai, on March 4–12, 2005. During the experiment, atmospheric sound levels in the 0.5–20 Hz frequency band were associated with large breaking ocean waves. The envelope of surf infrasound signals yields breaking wave periods comparable to those derived from nearshore sea surface elevation measurements. Our analysis confirms that individual plunging waves are partly responsible for the generation of surf infrasound. We demonstrate the potential to extract breaking wave period from a single, well sited infrasonic microphone. **Citation:** Aucan, J., D. Fee, and M. Garcés (2006), Infrasonic estimation of surf period, *Geophys. Res. Lett.*, *33*, L05612, doi:10.1029/2005GL025086.

1. Introduction

[2] In a companion paper, *Garcés et al.* [2006] summarizes previous work on surf infrasound and describes two experiments performed in the Hawaiian islands in January–March of 2005. The aim of these experiments was to help identify the processes that produce surf infrasound and further develop the capability to use infrasound arrays to characterize surf dynamics. *Garcés et al.* [2006] corroborate the relationship between the infrasonic amplitude and swell height and conclude that low-frequency airborne sound can be used to monitor the energetics, spatial distribution, and temporal variability of different types of breaking ocean waves.

[3] In this paper we concentrate on the unprecedented ability to extract breaking ocean wave period from infrasonic time series. To investigate the generation of infrasound by surf waves, we use the simultaneous video, ocean bottom pressure, and infrasonic measurements of breaking waves observed at Polihale Beach during March 2005 [see *Garcés et al.*, 2006]. Its straight coastline and unobstructed exposure to the dominant wintertime northwest swells permitted the identification of a clear relation between infrasound signal levels and individual waves or sets of waves, yielding valuable insight into the physics of surf infrasound generation.

[1]Department of Oceanography, School of Ocean and Earth Science and Technology, University of Hawaii at Manoa, Hawaii, Honolulu, Hawaii, USA.
[2]Hawaii Institute of Geophysics and Planetology, School of Ocean and Earth Science and Technology, University of Hawaii at Manoa, Honolulu, Hawaii, USA.

0094-8276/06/2005GL025086$05.00

2. Polihale

[4] Polihale Beach, on the NW coast of Kauai, Hawai'i, is a 4 km long, straight sandy beach oriented SW to NE, and backed by an 30 m high sand dune. It is fully exposed to swells generated by higher latitude winter storms. The offshore bathymetry is steep, with depths reaching 30 meters in 1 nautical mile. There is a 20 m deep shoal 2 nautical miles offshore running parallel to the beach, followed by an abrupt drop into the abyss. The island topography, as well as steep cliffs running parallel to the beach, block the prevailing ENE trade winds. Additional wind-noise reduction at the array site was provided by forest cover at the base of the cliffs. The Polihale area is accessible by all-terrain vehicle only and there is no regular cultural noise within a 10 km radius. A 60 m aperture infrasound array was deployed at Polihale on March 4–12, 2005. The array was located 250 m from the shoreline, in a forested area behind the sand dune. Three Seabird Electronics wave gauges (sbe 26) were deployed on the seabed along a line perpendicular to shore, at depths of 14, 18 and 22 m, and at a distance of 611, 765 and 1354 m from the coastline. The wave gauges recorded continuous ocean bottom pressure at 1 sample per second. The experiment sought to study large surf generated by low latitude winter storms in the North Pacific (Figure 1). These storms generate swells with dominant frequencies between 0.04 and 0.1 Hz. At all the wave gauge depths, these dominant frequencies are well below the high-frequency cutoff associated with the exponential depth attenuation of the ocean surface pressure. Due to its orientation, Polihale beach is sheltered from the high frequency ocean wind waves generated by the prevailing easterly trade winds, except near day 65 and 67 when wind waves were generated during brief southwesterly wind events. The favorable location, orientation, bathymetry, and exposure of the experimental site allowed us to concentrate on the radiation of infrasound by low frequency, high amplitude swells.

3. Estimating the Surf Infrasound Envelope

[5] We wish to find modulations of the surf infrasound envelope on the time scale of individual breaking ocean waves. In this paper, we only use data from one wave gauge to identify individual ocean waves near the surf zone. The pressure disturbance caused by wave-induced sea level variations decreases with depth. The pressure p at a depth z is defined by

$$p(z,k) = \rho g \zeta \frac{\cosh(k(h-z))}{\cosh(kh)} \quad (1)$$

where ρ is the water density, g is gravity acceleration, ζ is the sea surface elevation, h is the water depth, and k is the wave number, related to the wave frequency ω by the

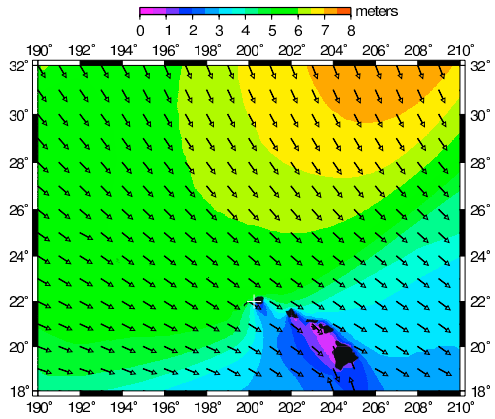

Figure 1. Location of the experiment (cross) and wave height and direction on day 64.

dispersion relation $\omega^2 = gk \tanh(kh)$. In order to remove the mean depth and the tidal variability, the bottom pressure time series was demeaned and detrended. A Fourier analysis was performed on each hour-long bottom pressure record to obtain the bottom pressure Fourier coefficient $F_p(\omega)$. Using equation 1, the Fourier coefficients $F_p(\omega)$ were converted into Fourier coefficients of the sea surface elevation $F_\zeta(\omega)$ to calculate the variance of the sea surface elevation σ_ζ. A spectrogram is used to visualize the evolution of the sea-surface elevation spectrum with time (Figure 2a). The significant wave height H_s (Figure 3b) was then computed as $H_s = 4\sqrt{\sigma_\zeta}$. The dominant frequency ω_p (or dominant period $T_p = 1/\omega_p$) is the frequency ω for which $F_\zeta(\omega)$ is maximum (Figure 3a).

[6] In this paper, we investigate in more detail the relation between individual breaking waves and infrasound generation in the 4–10 Hz band (the surf infrasound). To this end, we analyze the modulation of the surf infrasound envelope. Envelope fluctuation is a feature of all acoustic signals, except for pure tones and frequency-modulated

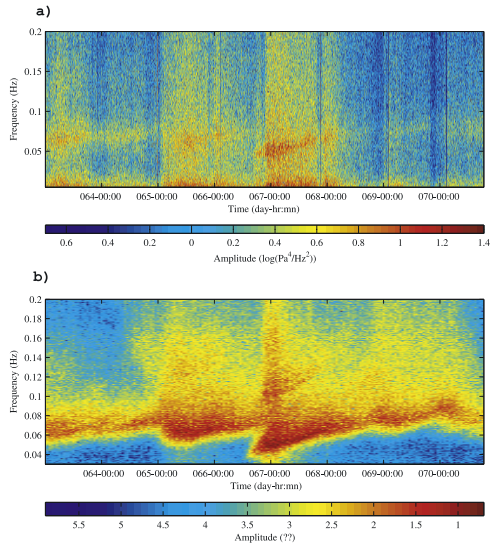

Figure 2. (a) Spectrogram of the envelope of the infrasound signal in the 4–10 Hz band, and (b) spectrogram of the sea-surface elevation, using 3600 seconds windows.

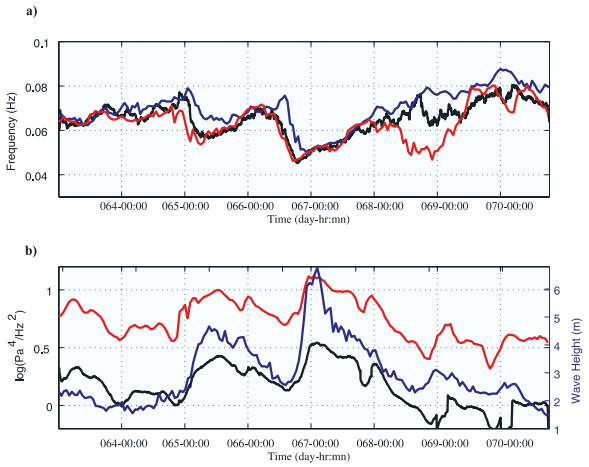

Figure 3. (a) Dominant frequency and (b) amplitude of the sea-surface elevation (blue) and the surf infrasound envelope, using a 3600 s window (red), and a 256 s window (black).

tones [*Ewert et al.*, 2002]. We use only the infrasound signal $S_i(t)$ measured at the array's central element. We calculated the Fourier coefficient $F_i(\omega)$ for 2 second segments with a 50 percent overlap.

[7] For each segment, the envelope $Env(t)$ of the surf infrasound signal is calculated by summing the infrasound spectral amplitudes of all frequencies between 4 and 10 Hz: $Env(t) = \sum_{\omega=4}^{\omega=10} F_i(\omega)$. The envelope time series, sampled at 1 second, was then treated in the same way as the sea-surface elevation time series to produce a spectrogram of the surf infrasound envelope (Figure 2b) using 3600 seconds samples. Individual spectra of the surf infrasound envelope show a peak at the same frequency as the incoming ocean waves, and this is peak is statistically significant (for example the peak at 0.07 Hz on Figure 4). The good agreement between the peak frequency of the incoming ocean waves and the peak frequency of the 4–10 Hz infrasound envelope (Figure 4) suggests that the generation of infrasound in the 4–10 Hz band is due to individual breaking waves. A forthcoming paper will use the wave gauge data to develop a clearer temporal correlation between infrasound levels and individual breaking waves.

[8] The surf envelope spectrogram was then used to calculate the mean surf infrasound intensity (Figure 3b), and the dominant frequency (Figure 3a), that is, the frequency at which the surf infrasound signal in the 4–10 Hz band is modulated.

[9] A spectrogram of the sea-surface elevation is useful to identify the arrival of a swell. Typically, a new swell arrival starts with a low dominant frequency, then the dominant frequency increases with time at a rate depending on the distance from the swell generating storm and the fetch characteristics (Figure 2a). During the experiment, several energetic low-frequency (0.04–0.1 Hz) swells were recorded, some reaching wave heights over 6 m in 14 m water depth (Figure 3a). These swells are generated by high latitude storms in the North Pacific (Figure 1). During days 65 and 67, the atmospheric circulation from one of these storms extended sufficiently far equatorward to affect the wind field at the study site. During this period, commonly

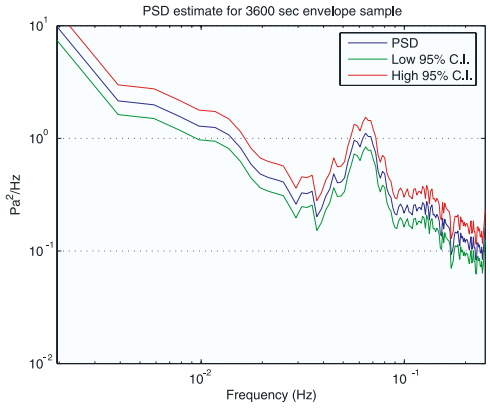

Figure 4. Example of spectrum of the envelope of the infrasound signal in the 4–10 Hz band, from Figure 2 on day 64, with 95% confidence intervals.

referred to as Kona winds in Hawaii, winds turned to a more westerly direction. These winds created locally generated high frequency waves (0.1–0.2 Hz) in addition to the energetic low frequency swell generated further upstream (Figure 2a).

[10] Around Day 67, a secondary peak appears in the sea-surface spectrogram, at exactly twice the dominant frequency. This secondary peak could be either due to a secondary, locally generated, high-frequency wind swell, or the superposition of an incident and a reflected low-frequency swell. Given that the secondary and the primary peaks show the same evolution with time, and given the visual observations of energetic "backwash" events when a reflected wave crest collides with an incoming crest, we suggest that this secondary peak is due to the primary swell energy being reflected at the beach. Such coastal reflections have been identified as the dominant source of microseismic signals at land-based seismic stations [*Bromirski and Duennebier*, 2002], and are also likely a source of microbaroms.

[11] The spectrogram of the surf infrasound envelope illustrates the modulation of the surf infrasound signal, and coincides very well with the spectrogram of the sea surface elevation for frequencies between 0.04 and 0.1 Hz (Figure 2). In both spectrograms, the individual swells can be identified by the characteristic abrupt increase in energy at low frequency, followed by a slow energy decrease associated with an increasing dominant frequency (days 65–66 and days 67–69 on Figure 2). The similarity between the spectrogram of the sea-surface elevation and the envelope of the surf infrasound signal is confirmed when extracting their respective amplitude and dominant frequency (Figure 3). The correlation coefficient (r-value) for the amplitude (Figure 3a) is 0.58 and 0.76 for the dominant period (Figure 3b). However, the infrasound envelope spectrogram shows increased energy in the low frequency end that does not appear related to similar low-frequency sea surface displacements. Figure 3 also shows the period and amplitude derived from the infrasound envelope spectrogram using 256 s windows. These results match the wave gauge periods better on days 69 and 70, when the ratio of short period to long period ocean wave energy was high. The correlation is also improved when using a shorter 256 s window compared to using a 3600 s window (correlation of 0.92 and 0.79 for the amplitude and period, respectively, when using a 256 s window). Later work will explore in more detail the use of different processing parameters for different sea states and wave types.

4. Infrasonic Surf Monitoring

[12] *Garcés et al.* [2006] and this study show that surf generates infrasound in the 0.5–20 Hz frequency band. Our experiments in Hawaii have demonstrated that waves breaking on a rocky shelf or cliff and plunging breakers trapping and releasing air can produce infrasound. Based on video synchronous with the acoustic data, we also postulate that large-scale whitewater bores produced during and after wave breaking may produce infrasound. The steep, sandy beach at Polihale favored plunging breakers over spilling breakers, and numerous visual observations were made of trapped air ejection after the wave plunged. We found that the envelope of the infrasound signal is modulated at the frequency of individual waves, consistent with the hypothesis that plunging breakers are predominantly responsible for the surf infrasound. After breaking, the remaining ocean wave energy remained in the bore until the shoreline. The surf zone was sufficiently wide for multiple bores to exist while new waves broke, with some waves breaking again after reforming. It is possible that the low frequency modulation of the infrasound signal (near 0.01 Hz) may be related to the propagating bores. In this manuscript we demonstrate the potential to estimate breaking wave period from a single infrasound microphone. We conclude that, with proper site selection, it is possible to use infrasound as a low-cost, real-time remote sensing tool for regional surf monitoring.

[13] **Acknowledgments.** This work was funded by the National Defense Center of Excellence for Research in Ocean Sciences (CEROS). CEROS is funded by the Defense Advanced Research Projects Agency (DARPA) through grants to and agreements with the Natural Energy Laboratory of Hawaii Authority (NELHA), an agency of the Department of Business, Economic Development and Tourism, State of Hawaii. This report does not necessarily reflect the position or policy of the Government, and no official endorsement should be inferred. This CEROS research project was conducted in collaboration with BBN Technologies. The deployment and recovery of the wave gauges was achieved in less than ideal sea conditions by divers Jamison Gove, Oliver Vetter and Shawn Fujimoto. Captain Linda Marsh was essential in providing expert knowledge of boating in the area. The authors are grateful to Ronald Hoeke (NOAA/CRED) who promptly provided the replacement wave gauges used in this study after the loss of our gauges during shipping.

References

Bromirski, P. D., and F. K. Duennebier (2002), The near-coastal microseism spectrum: Spatial and temporal wave climate relationships, *J. Geophys. Res.*, *107*(B8), 2166, doi:10.1029/2001JB000265.

Ewert, S. D., J. L. Verhey, and T. Dau (2002), Spectro-temporal processing in the envelope-frequency domain, *J. Acoust. Soc. Am.*, *112*(6), 2921–2931.

Garcés, M., J. Aucan, D. Fee, P. Caron, M. Merrifield, R. Gibson, J. Bhattacharyya, and S. Shah (2006), Infrasound from large surf, *Geophys. Res. Lett.*, *33*, L05611, doi:10.1029/2005GL025085.

J. Aucan, Department of Oceanography, School of Ocean and Earth Science and Technology (SOEST), University of Hawaii, Honolulu, HI 96822, USA. (jaucan@soest.hawaii.edu)

D. Fee and M. Garcés, Hawaii Institute of Geophysics and Planetology, School of Ocean and Earth Science and Technology (SOEST), University of Hawaii at Manoa, Honolulu, HI 96822, USA.